Alexandria Engineering Journal (2018) 57, 3727–3735

HOSTED BY

Alexandria University

Alexandria Engineering Journal

www.elsevier.com/locate/aej
www.sciencedirect.com

ORIGINAL ARTICLE

Photocatalytic decolorization of methylene blue using TiO_2/UV system enhanced by air sparging

M.H. Abdellah [a,*], S.A. Nosier [a], A.H. El-Shazly [b], A.A. Mubarak [a]

[a] *Chemical Engineering Department, Faculty of Engineering, Alexandria University, Alexandria, Egypt*
[b] *Chemical and Petrochemicals Engineering Department, Egypt-Japan University of Science and Technology (E-JUST), New Borg El Arab City, Alexandria, Egypt*

Received 25 July 2017; revised 31 March 2018; accepted 28 July 2018
Available online 16 November 2018

KEYWORDS

Photocatalysis;
TiO_2;
Air sparging;
Methylene blue;
Ultraviolet

Abstract In this work, the photocatalytic degradation of wastewater containing an organic dye (Methylene Blue) was investigated in a slurry-type reactor enhanced by air sparging. Commercial TiO_2 was used as the photocatalyst which was activated using ultraviolet irradiation. The effects of initial dye concentration, photocatalyst loading, solution pH and air's superficial velocity on the degradation efficiency were evaluated. The degradation efficiency of the dye increased with increasing the pH of the solution and decreasing the initial dye concentration. Moreover, increasing the catalyst loading up to 1 g/l showed an improvement in the degradation efficiency. However, the efficiency deteriorated with a further increase in the catalyst loading. Introducing air into the reaction medium in the form of micro-bubbles significantly improved the degradation efficiency by providing oxygen molecules required for the oxidation reaction. Furthermore, these air bubbles created turbulence in the reaction medium, which resulted in the enhancement of the mass transfer rate of dye molecules from the solution bulk to the catalyst surface with a subsequent increase in the degradation efficiency. A complete decolorization of 10 ppm dye solution was achieved in the neutral solution ($pH = 7$) with a catalyst loading of 1 g/l and an air superficial velocity around 2 cm/s. The effect of the air superficial velocity on the degradation reaction kinetics was investigated and the reaction was found to follow the pseudo second order rate law.

1. Introduction

Wastewater effluents from industries, such as textile, printing, paints and leather tanning, contain a large variety of organic compounds, which cause serious problems to the environment [1,2]. Dyes are one of these harmful organic pollutants and are released mainly from the textile and painting industries to the environment [3,4]. When these dyes hydrolyse and react with other pollutants present in the wastewater effluents, they produce lethal carcinogenic byproducts, which not only threaten the aquatic environment but also the health and wellbeing of human beings [4]. Methylene blue (MB) is a basic dye, which is typically used for dyeing wool and silk. It is also used for medical purposes to inspect some diseases. Discharging of wastewater effluents, which are contaminated with MB, to feed

---

[*] Corresponding author.
E-mail address: m.hussein2010@alexu.edu.eg (M.H. Abdellah).

Peer review under responsibility of Faculty of Engineering, Alexandria University.

https://doi.org/10.1016/j.aej.2018.07.018
1110-0168

Nomenclature

λ_{max}	maximum wavelength (nm)	M.wt	molecular weight
C_o	initial dye concentration (mg/l)	UV	ultraviolet
C_t	dye concentration at time t (mg/l)	MB	methylene blue
q_t	adsorption capacity at time t (mg/g)	R^2	coefficient of determination
q_e	equilibrium adsorption capacity (mg/g)	h^+	positive hole
K_1	pseudo first order rate constant (min^{-1})	e^-	free electron
K_2	pseudo second order rate constant (g/min.mg)	$_{VB}$	valence band
V_{air}	air superficial velocity (cm/s)	$_{CB}$	conduction band
ΔE_{gab}	band gap energy (eV)		

water resources, such as rivers, lakes, and seas without efficient degradation results in harmful effects, such as burns of eye, nausea, vomiting, and diarrhea [5]. Therefore, finding an effective treatment method for wastewater containing dyes has become an important research goal.

Several treatment technologies have been developed for the decolorization and degradation of dyes in wastewater effluents. These technologies are classified according to the principle of remediation into (1) physical methods, such as adsorption [6], reverse osmosis [7], ultrafiltration [8] and ion exchange [9], (2) chemical methods, such as chlorination and ozonation [10], and (3) biological methods, such as aerobic and anaerobic treatments [4,5,11]. Most of these traditional techniques remove pollutants by transferring them from one phase to another without converting them into environmentally-friendly end products. Therefore, they create another contaminated material, which requires further treatment and hence, adds an extra cost to the overall degradation process [12]. Advanced oxidation processes (AOPs) such as Fenton, photo-Fenton catalytic reactions, UV/H_2O_2 and UV/O_3 have proved to be sufficiently effective alternatives for the treatment of wastewaters containing dyes [12,13]. Among them, the heterogeneous photocatalytic oxidation has received a growing attention over the last two decades.

In this process, a semiconductor, which is either a metal oxide, such as WO_3, ZnO, CeO_2, Nb_2O_3, Fe_2O_3, SnO_2 and TiO_2 or a chalcogenide, such as ZnS, CdTe, ZnSe, and CdSe, is used as a photocatalyst [14]. Compared with the conventional processes used for the removal of organic contaminants, the photocatalytic oxidation has shown the highest efficiency, as it leads to a complete mineralization of a wide range of organic pollutants. Another advantage of the process is that it produces harmless compounds, such as CO_2, H_2O and mineral acids [3,13,15].

Semiconductors are characterized by a specific electronic structure of a filled valence band and an empty conduction band. The difference between the energy of valence and conduction bands is known as the band gap energy. This band gap energy ranges from 3 to 3.5 eV depending on the type of the semiconductor [11,16]. When the semiconductor is exposed to irradiation having an amount of energy equal to the band gap energy, the semiconductor atoms are excited, due to which, one electron jumps from the filled valence band to the empty conduction band. As a result, a free electron exists in the conduction band, while a positive hole is formed in the valence band [16]. This electron/hole pair can take various possible reaction routes [14]. After moving to the surface of the photocatalyst, the free electron may react with a reducing agent (electron acceptor), while the positive hole reacts with an oxidizing agent (electron donor) adsorbed on the surface. The free electron and the positive hole may recombine, which is undesirable and should be minimized for the sake of photocatalytic activity [17]. The overall photocatalytic activity of a particular semiconductor is measured based upon several factors, including chemical and physical stability of the semiconductor under irradiation, wavelength range required to activate the catalyst, selectivity of the reaction products and efficiency of the photocatalytic process [18]. Among various semiconductors, titanium dioxide represents a promising photocatalyst due to its unique chemical and biological stability, hydrophobicity, low price and availability [19,20]. However, the irradiation energy within the ultraviolet spectrum ($<10\%$ of the total solar irradiation) is required to activate the photocatalyst [21].

In the past, several studies have focused on investigating the photocatalytic activity of TiO_2 for the degradation of organic pollutants. Behpour et al. [22] studied the photocatalytic degradation of Yellow 24 using TiO_2 thin films under visible light and found that the degradation efficiency decreased with the increase in feed solution's flow rate. In another study, which focused on the degradation of different dyes (toluidine blue, safranin orange and crystal violet) using V_2O_5/TiO_2 hybrid photocatalyst subjected to UV light, Rauf et al. [23] observed an improvement in the decolorization efficiency with the increase in the amount of catalyst to a certain limit before it decreased with the further increase in the catalyst loading. Similar results were also reported by others [2,24]. Zhang et al. [25] reported a new method for the preparation of TiO_2 hollow nanospheres and evaluated their photocatalytic activity by the degradation of some organic dyes under UV irradiation. Compared with the commercial Degussa P25, the authors found that these TiO_2 hollow spheres showed a higher photocatalytic activity. Houas et al. [3] investigated the photocatalytic degradation of methylene blue using a TiO_2/UV system in an aqueous suspension under different experimental conditions and observed a complete demineralization (100%; 1000 min) of the dye molecules to environmentally-friendly by-products. As an attempt to improve the photocatalytic activity of titania under visible light, Haque et al. [26] synthesized La- and Mo-doped TiO_2 hybrid carbon nanospheres and found that 2% La and 1.5% Mo-doped TiO_2 showed the highest photocatalytic activity for the degradation of different chromophoric dyes. In a recent work, Kuyumcu et al. [27] evaluated the performance of TiO_2 doped with different metals

(Cu, Co, Ni, Mn, and Fe) for the photocatalytic decomposition of methyl orange and methylene blue under visible light irradiation. After 5 hr of continuous illumination, the degradation efficiencies for methyl orange and methylene blue were found to be 26% and 16%, respectively. Jaimy et al. [28] reported 74% decomposition of methylene blue (160 min) using Fe and Ce doped TiO_2 under visible light irradiation.

In the present study, a TiO_2/UV system was used for the degradation of MB in a photocatalytic reactor enhanced by air sparging. The effects of dye concentration, pH of the solution, photocatalyst dosage and superficial velocity of air on the degradation efficiency were investigated. The kinetics of the photocatalytic reaction was studied to determine the corresponding rate law of the reaction. Finally, the effect of air superficial velocity on the reaction kinetics was investigated.

2. Experimental part

2.1. Materials

All chemicals used in this work were of analytical grade and used without further purification. Commercial titanium dioxide (TiO_2; fine white powder) was purchased from Shanghai Yuejiang Titanium Chemical Manufacturer Co., Ltd., China, and was used as the photocatalyst. Methylene blue (M.wt of 319.86; molecular formula of $C_{18}H_{18}N_3SCl_3H_2O$; λ_{max} of 663–667 nm; cationic) was obtained from Chemjet (India) and was used for the preparation of the modeled wastewater. The pH of the wastewater was adjusted prior to each experiment using solutions of NaOH (Gateway; 97%) and H_2SO_4 (SDFCL; 98%). Distilled water was used in all the experiments.

2.2. Experimental setup

Fig. 1 shows the schematic of the setup used to study the photocatalytic degradation of the wastewater containing MB. The setup consisted of a cylindrical plexiglass photocatalytic reactor with the height and inner diameter of 50 cm and 5 cm, respectively. At the bottom, the cylinder was fitted with a 0.5-cm thick sintered glass disk of 40–100 μm pore size (G-2) to create micro air bubbles. The reactor was irradiated by placing a UV lamp (GERNICIDAL; Hg; 15 W), which was concentric with the plexiglass cylinder to ensure a uniform distribution of the UV light on the reaction medium. In order to prevent the interference of UV irradiation with the visible light from the surrounding and to maximize the use of UV irradiation, the outer surface of the cylinder was covered with a reflective aluminium foil. Atmospheric air at ambient temperature (25±2) °C was fed from the bottom of the reactor through the sintered glass disk. A reciprocating compressor (Italtecnica; 1.5 HP) was used to feed the air. The flow rate was controlled using a needle valve and was measured using a calibrated rotameter (TEFLON).

2.3. Methods and analysis

The modeled wastewater was prepared by diluting a 1000 ppm stock dye solution. 250 ml of the prepared wastewater was placed inside the reactor after adjusting the pH to a required value using a portable pH meter (NEEWAR). After that, the TiO_2 powder was added to the dye solution inside the reactor and air was bubbled through the reaction media for 10 min to ensure a good dispersion of the catalyst and to reach the adsorption equilibrium conditions. The UV light was irradi-

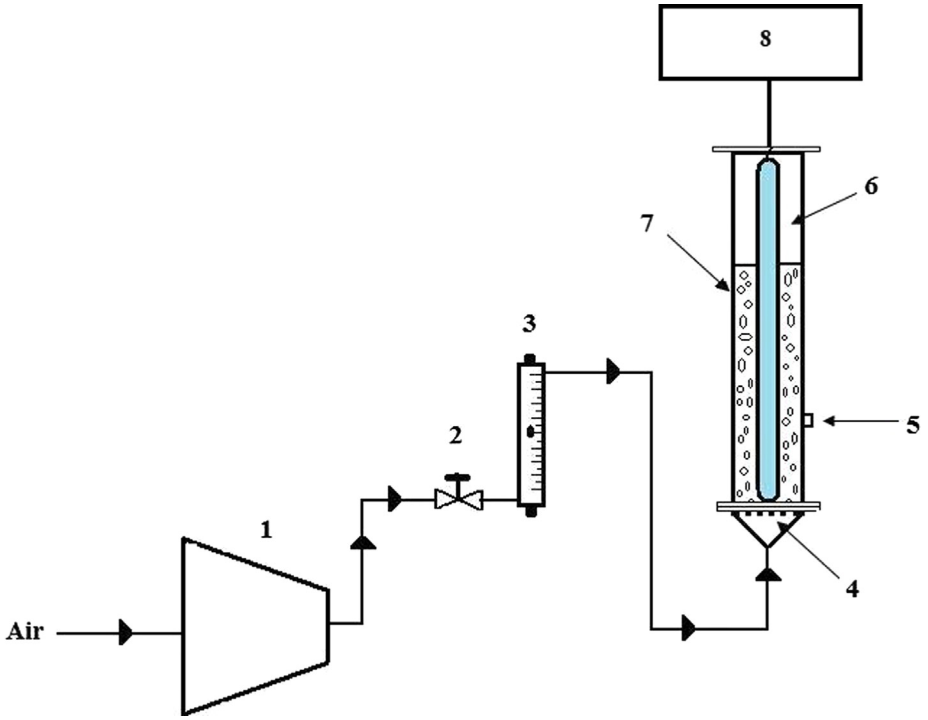

Fig. 1 Experiment setup. (1) Air compressor. (2) Flow control valve. (3) Air rotameter. (4) Sintered glass disk (diffuser). (5) Sampling port. (6) UV lamp 254 nm. (7) Reflective foil. (8) Power source.

ated for a certain period of time to activate the catalyst, thus resulting in the degradation of the dye. A 3-ml sample was collected every 5 min for further analysis. Prior to measuring the dye concentration, the residual TiO_2 in the sample was separated using a tabletop centrifuge (DAIGGER, USA). The dye concentration was determined from a standard curve using the absorbance values measured by the UV–visible spectrophotometer ((UNICO, USA), which was adjusted at 664 nm (wavelength corresponding to the maximum absorption of MB). The effects of initial dye concentration, solution pH, catalyst loading and air superficial velocity on the process performance were investigated. The process efficiency was evaluated in terms of the percentage color removal of the dye, which was calculated using Eq. (1).

$$\%\ \text{color removal} = \frac{C_o - C_t}{C_o} \times 100 \qquad (1)$$

where C_o and C_t are the initial and the dye concentration at time t (measured as mg/l (ppm)).

3. Results and discussion

3.1. Characterization of the TiO_2 photocatalyst

Characteristics of the photocatalyst, which constitute the main factors affecting the degradation efficiency, were considered for analysis. Titanium dioxide has three different crystal structures, known as brookite, rutile, and anatase, which has the highest photocatalytic activity. The crystal structure of TiO_2 used in the current study was determined using X-ray diffractometer (SCHIMADZU model, Japan) using Cu-Kα X-rays of wavelength (λ) = 1.5406 Å. The pattern was collected in the range of 4–140° 2θ with a scanning step of 0.02° in a continuous scanning mode. The X-ray diffraction pattern of the sample is presented in Fig. 2. The Strong diffraction peaks at 25.27° and 48.01°, which are in agreement with the JCPDS card no. 21-1272, confirm the anatase crystal structure of TiO_2 [29].

The particle size was estimated from the particle size distribution analysis conducted using an N5 Submicron particle size analyzer, BeckMan Coulter, which used water as the diluent at a scattering angle of 90° (Fig. 3). The mean particle diameter was found to be around 180 nm. The surface morphology of TiO_2 was visualized using a scanning electron microscope (SEM; JOEL Japan, Model JSM-636OLA) and is presented in Fig. 4. It can be seen that the particles have a spherical shape with an average diameter ranging from 120 to 180 nm, which agrees well with the particle size analysis. Additionally, it can be seen that the particles agglomerate to form a rough porous texture.

3.2. Factors affecting the photocatalytic reaction

3.2.1. Effect of the solution pH

According to the nature of dyes (either cationic, anionic or neutral), the pH of dying process varies to enhance the process and ensure a strong adhesion of dye molecules to the object to be colored. The pH of the wastewater is considered one of the main factors that determines the appropriate remediation process. For heterogeneous solid/liquid reactions, such as the photocatalytic reaction, the reaction proceeds through several steps. The reactants, which are the dye molecules in the present study, diffuse from the bulk of the solution to the surface of the catalyst, which acts as an adsorbent to hold the reactants. When the system is irradiated with a suitable light having sufficient energy to activate the catalyst, the degradation reaction begins. After the completion of the reaction, the reaction products are desorbed from the catalyst surface and diffuse back into the solution's bulk. The pH is considered the main parameter affecting the adsorption process due to its impact on the surface charge of the catalyst. The effect of the solution pH within the range of 3–7 on the degradation efficiency was investigated. Fig. 5 shows the percentage color removal with respect to the reaction time for the degradation of MB at various solution pH values. The net effect of the solution pH under different experimental conditions is exhibited in Fig. 6. An increase in the degradation efficiency, expressed as the percentage color removal, was observed with increasing the pH from 3 to 7. This may be attributed to the basic nature of MB combined with the amphoteric properties of the TiO_2. In acidic solutions with pH values less than 5.8, the surface of TiO_2 particles gains a positive charge, while at pH 6.8, it gains a negative charge. The pH range (5.8–6.8) is known as the zero point of charge where the surface of TiO_2 particles has no

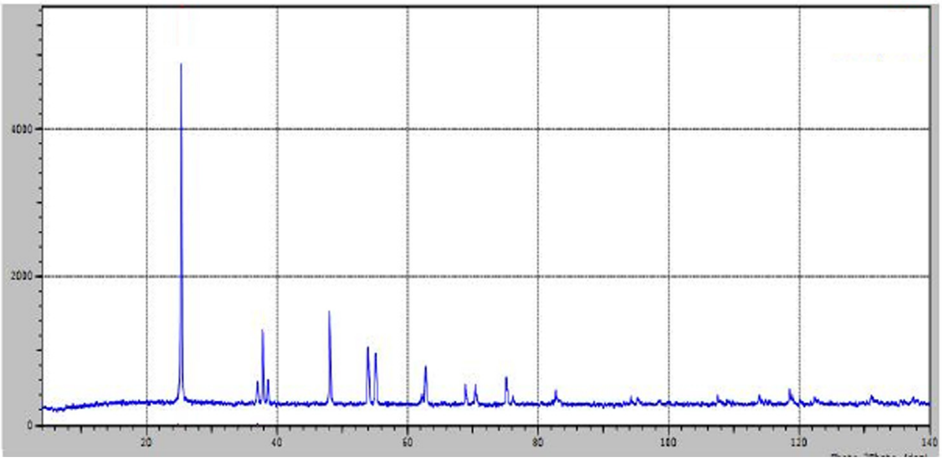

Fig. 2 XRD pattern for the TiO_2 photocatalyst used in the current study.

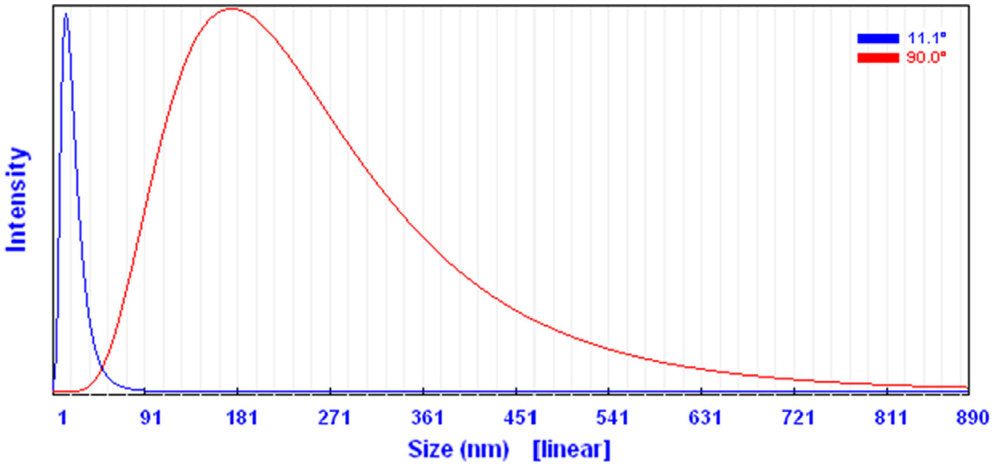

Fig. 3 Mean particle size of TiO_2 used in the current study.

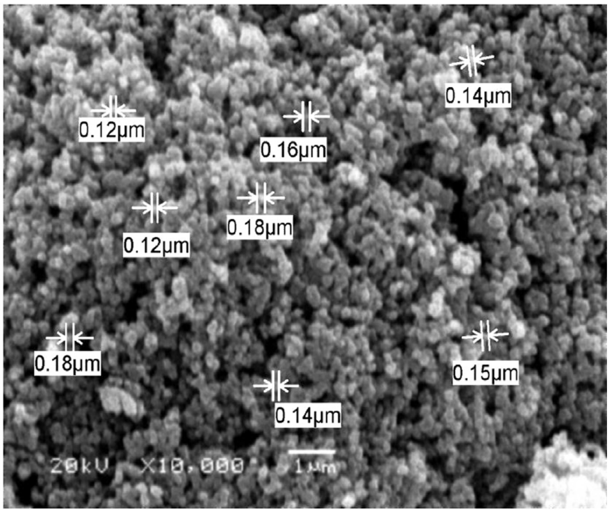

Fig. 4 SEM image of the TiO_2 used in the current study.

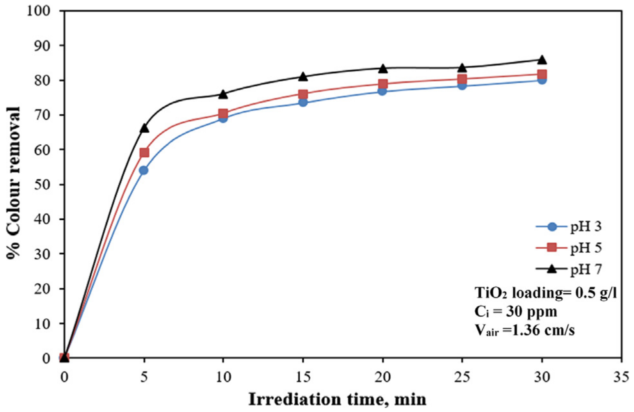

Fig. 5 Percentage color removal- time profile for different solution pH values.

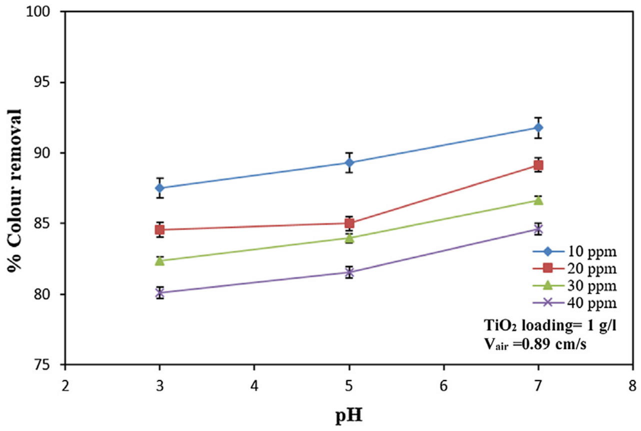

Fig. 6 Effect of solution pH on the percentage color removal at different experimental conditions.

charge [3,5,30,31]. Accordingly, the MB molecules, which gain a positive charge after dissolution in water, will be adsorbed more and faster at the pH higher than 6.8 with a subsequent increase in the percentage color removal.

3.2.2. Effect of initial dye concentration

Wastewater effluents disposed after the completion of the dying process have different dye concentrations depending on the required color intensity of the final product. Variation in the color intensity (dye concentration) affects the intensity of light passing through the reaction medium to reach the surface of the photocatalyst. Accordingly, investigating the effect of dye concentration on the photocatalytic process is of a great significance. The influence of the initial dye concentration on the decolorization of MB was investigated within a broad range of concentration (10–40 ppm). The effect of initial dye concentration on the degradation efficiency is presented in Figs. 7 and 8. A significant decrease in the percentage color removal was observed with the increase in the initial dye concentration. This may be attributed to the coverage of catalyst's active sites due to the increased adsorption of dye molecules. Consequently, the generation of active $OH^{\bullet}$ radicals responsible for the degradation reaction was suppressed. Another possible reason is the screening effect of the UV light, which increases with the increase in the intensity of the color (higher

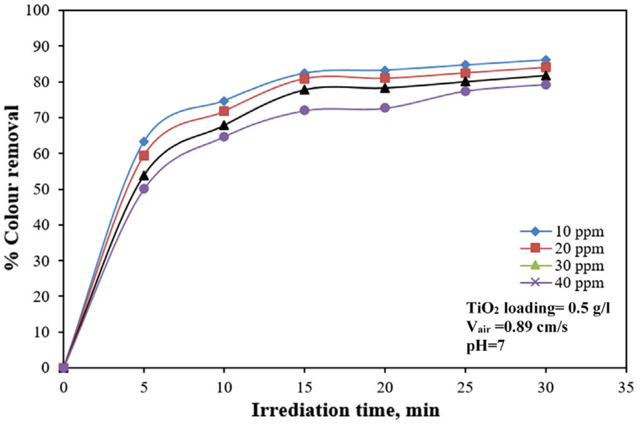

Fig. 7 Percentage color removal - time profile for different initial dye concentrations.

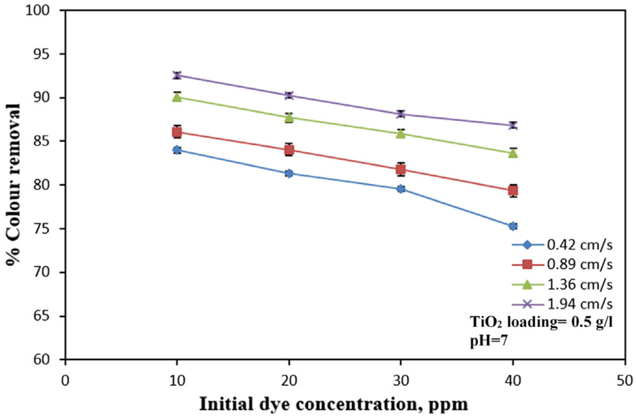

Fig. 8 Effect of initial dye concentration on the percentage color removal under different experimental conditions.

dye concentration). The screening of UV light results from the absorption of a fraction of UV light by the chromophores of the dye molecules. Therefore, less photon's energy reaches the active sites on the catalyst, which results in lower number of $OH^{\bullet}$ produced. Moreover, the intermediate compounds formed during the degradation process increase with the increase in the initial dye concentration and might consume some active radicals that are supposed to react with the dye molecules. As a result, the overall decolorization efficiency decreases [5,13,30].

3.2.3. *Effect of TiO_2 dosage*

Determination of the optimum amount of catalyst loading is a substantial stage in scaling up the photocatalytic process as it affects the economics of the process as well as the downstream processing to separate the photocatalyst from the reaction medium. The effect of TiO_2 loading on the degradation of MB was studied within the range of 0.5–2 g/l under different experimental conditions. The effect of catalyst's loading on the decolorization efficiency is depicted in Figs. 9 and 10. It can be seen that the amount of TiO_2 added to the reaction medium had a significant effect on the process efficiency. The percentage color removal increased with the increase in TiO_2 loading, and was maximum for 1 g TiO_2 /l. Beyond that,

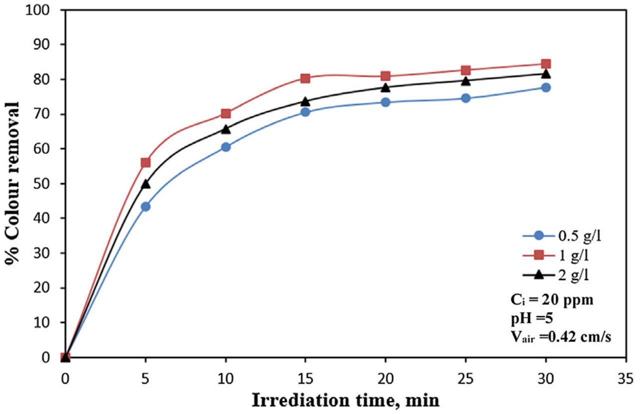

Fig. 9 Percentage color removal- time profile for different TiO_2 loadings.

the removal percentage decreased with a further increase in the TiO_2 dosage. The observed increase in the decolorization efficiency is explained by the increase in the (number) density of the catalyst's active sites, which in turn results in the formation of more active radicals (hydroxyl and superoxide) that initiate the degradation reaction. At higher catalyst loading, the TiO_2 particles act as a barrier for the incident UV irradiation and deter its arrival to some particles. Another possible reason is the agglomeration of the catalyst nanoparticles, which is favored by their high surface energy and surface area. Therefore, the effective surface area of the catalyst decreases and a reduction in the decolorization efficiency is expected.

3.2.4. *Effect of air superficial velocity*

During the photocatalytic reaction, air acts as a promoter by introducing molecular oxygen to the system. These oxygen molecules react with the free electrons, which are formed at the active sites on the catalyst surface upon UV irradiation. As a result, more hydroxyl radicals (the oxidant of the dye molecules) are formed according to the proposed degradation mechanism (Eqs. (2)–(9))[4].

$$TiO_2 + \Delta E_{gab}\,(UV) \rightarrow TiO_2\,(e^-{}_{CB} + h^+{}_{VB}) \tag{2}$$

$$TiO_2\,(h^+{}_{VB}) + H_2O \rightarrow TiO_2 + H^+ + OH^- \tag{3}$$

$$TiO_2\,(h^+{}_{VB}) + OH^- \rightarrow TiO_2 + OH^{\cdot} \tag{4}$$

$$TiO_2\,(e^-{}_{CB}) + O_2 \rightarrow TiO_2 + O_2^{\cdot -} \tag{5}$$

$$O_2^{\cdot -} + H^+ \rightarrow HO_2^{\cdot} \tag{6}$$

$$2HO_2^{\cdot} \rightarrow H_2O_2 + O_2 \tag{7}$$

$$H_2O_2 + e^- \rightarrow OH^- + OH^{\cdot} \tag{8}$$

$$\text{Dye (MB)} + OH^{\cdot} \rightarrow \text{degradation products} \tag{9}$$

The effect of the superficial velocity of the sparging air on the degradation of MB was investigated within the range of 0.42–1.94 cm/s and the results are presented in Figs. 11 and 12

A significant increase in the percentage color removal was observed with the increase in the air superficial velocity within

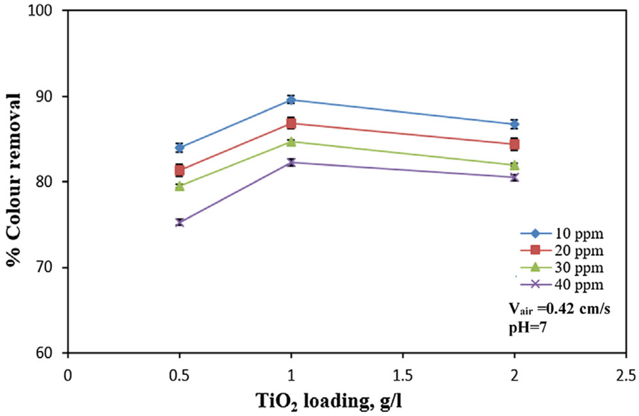

Fig. 10 Effect of TiO_2 loading on the percentage color removal under different experimental conditions.

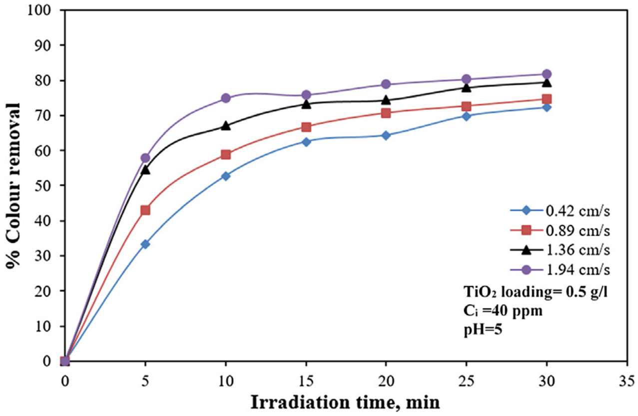

Fig. 11 Percentage color removal- time profile for different catalyst loadings.

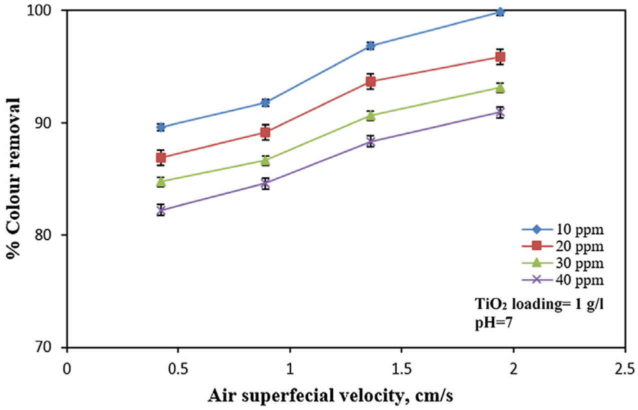

Fig. 12 Effect of air superficial velocity on the percentage color removal under different experimental conditions.

the experimental conditions used in the current study. Other than promoting the formation of active $OH^\bullet$ radicals, increasing the air superficial velocity results in an improvement in the mobility and diffusivity of dye molecules towards the catalyst active sites. Furthermore, the micro air bubbles flowing through the reaction medium at high velocity eliminate the potential coalescence and agglomeration of the TiO_2 nanoparticles, thus providing a bigger active surface area of the catalyst, which increases the process efficiency.

3.3. Kinetics of the photocatalytic degradation of MB

Facilitation of the large-scale implementation of photocatalytic processes requires understanding the kinetics of the reactions and finding their rate laws. The concentration-time data obtained in this work was used to find the appropriate kinetics for the photocatalytic degradation of MB enhanced by air sparging. Since the photocatalytic process is considered as a heterogeneous reaction, which encompasses solid, liquid and gas phases, the concentration-time data were fitted according to the integral forms of the pseudo first order (Lagergren's rate law; Eq. (10)) and the pseudo second order rate laws (Eq. (11)) [32].

$$\mathrm{Ln}\frac{(q_e - q_t)}{q_e} = -K_1 t \tag{10}$$

$$\frac{t}{q_t} = \frac{1}{K_2 q_e^2} + \frac{t}{q_e} \tag{11}$$

where q_t and q_e are the adsorption capacities (mg/g) at time t and at equilibrium, respectively, K_1 represents the pseudo first order rate constant (min^{-1}) and K_2 represents the pseudo second order rate constant (g/mg. min). Fig. 13 shows the pseudo first order fitting, while the results of the curve fitting for pseudo second order are presented in Fig. 14 for different air superficial velocities. For each of the fittings, the reaction rate constants and the coefficients of determination, which is a measure of the quality of the fitting, are compared in Table 1. Although there is a slight difference between the coefficients of determination of both presumed rate laws, it can be concluded that the degradation of MB in a slurry-type reactor enhanced by air sparging can be described by the second order reaction kinetics.

The correlation between the air superficial velocity and the reaction rate constant was obtained by plotting log (K_2) against log (V_{air}) (see Fig. 15). The increase in the air superficial velocity increases the reaction rate according to Eq. (12). As mentioned earlier, with increasing air superficial velocity

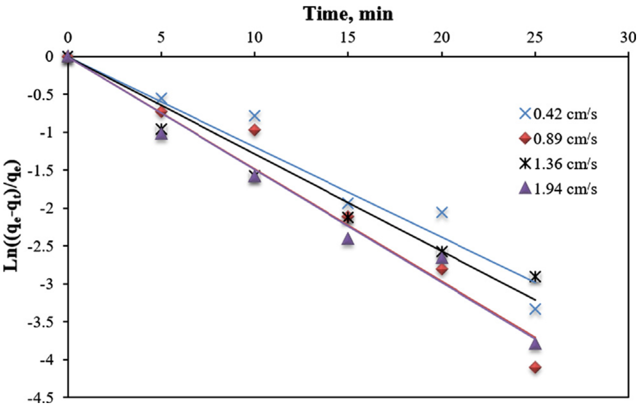

Fig. 13 Pseudo first order fitting of the photocatalytic degradation of MB under different air superficial velocities.

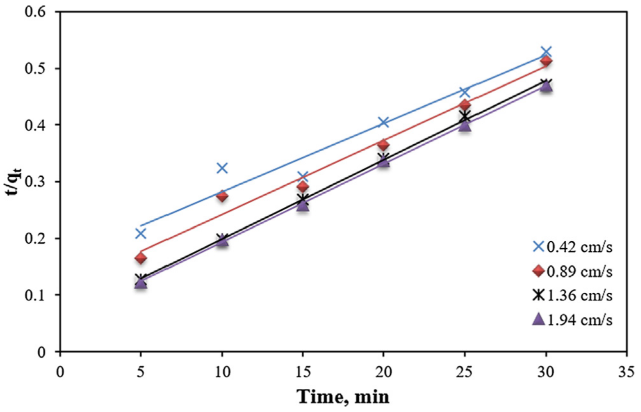

Fig. 14 Pseudo second order fitting of the photocatalytic degradation of MB under different air superficial velocities.

Table 1 Reaction rate constants for the photocatalytic degradation of MB estimated from pseudo first and second order rate laws with the corresponding coefficients of determination.

Rate law	V_{air} (cm/s)	Rate constant (K)	R^2
Pseudo first order (Lagergren's rate law), Eq.10	0.42	0.1192 (min^{-1})	0.944
	0.89	0.148	0.960
	1.36	0.128	0.946
	1.94	0.149	0.975
Pseudo second order, Eq. 11	0.42	8.88×10^{-4} ($g\ min^{-1}\ mg^{-1}$)	0.953
	0.89	1.53×10^{-3}	0.979
	1.36	3.32×10^{-3}	0.999
	1.94	3.46×10^{-3}	0.999

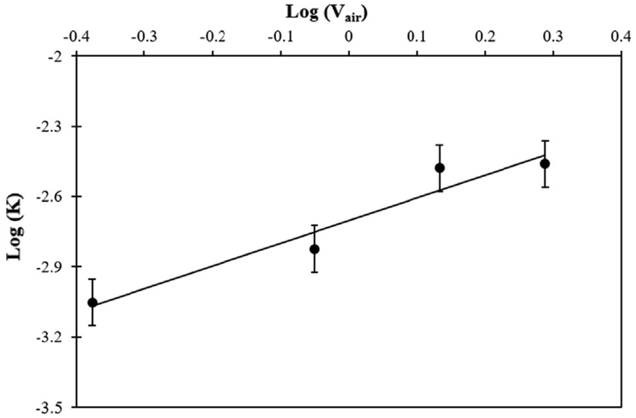

Fig. 15 Graphical determination of the correlation between the reaction rate constant and the air superficial velocity.

the amount of oxygen supplied to the reaction media increases, which subsequently increases the number of active radicals responsible for the degradation reaction.

$$K_2\left(\frac{g}{\min .mg}\right) = 1.984^{-3} V_{air}^{0.9669}\left(\frac{cm}{s}\right) \tag{12}$$

The rate law of the of the photocatalytic degradation of MB in the system studied in the current work can be expressed in terms of the air superficial velocity and the adsorption capacity according to Eq. (13).

$$\frac{t}{q_t} = \frac{1}{1.984^{-3} V_{air}^{0.9669}\left(\frac{cm}{s}\right) q_e^2} + \frac{t}{q_e} \tag{13}$$

4. Conclusions

In a modeled wastewater, methylene blue was effectively decolorized using a photocatalytic technique, which used TiO_2/UV system enhanced by air sparging. The optimum catalyst loading was found to be 1 g/l. The results showed that the percentage color removal increased with increasing the solution pH. Moreover, the percentage color removal increased with the decrease in dye concentration under all experimental conditions used in the current study. The photocatalytic technique is favorable at low MB concentrations as the percentage removal decreased with increasing the initial dye concentration. Air contributed efficiently to enhancing the degradation reaction, whereas complete decolorization was achieved by increasing the air superficial velocity from 0.42 cm/s to 1.96 cm/s under optimum reaction conditions (pH = 7; catalyst loading = 1 g/l; initial dye concentration = 10 ppm). The kinetics of the reaction was studied and found to follow the pseudo second order rate law. Furthermore, increasing air's superficial velocity resulted in an increase in the reaction rate.

Acknowledgments

This work was supported by the Chemical Engineering Department, Faculty of Engineering, Alexandria University, Egypt.

References

[1] M. Barjasteh-Moghaddam, A. Habibi-Yangjeh, Effect of operational parameters on photodegradation of methylene blue on ZnS nanoparticles prepared in presence of an ionic liquid as a highly efficient photocatalyst, J. Iran. Chem. Soc. 8 (2012) S169–S175.

[2] S.B. Gajbhiye, Photocatalytic degradation study of methylene blue solutions and its application to dye industry effluent, IJMER 2 (2012) 1204–1208.

[3] A. Houas, H. Lachheb, M. Ksibi, E. Elaloui, C. Guillard, J.-M. Herrmann, Photocatalytic degradation pathway of methylene blue in water, Appl. Catal. B Environ. 31 (2001) 145–157.

[4] U.G. Akpan, B.H. Hameed, Parameters affecting the photocatalytic degradation of dyes using TiO2-based photocatalysts: a review, J. Hazard. Mater. 170 (2009) 520–529.

[5] M. Salehi, H. Hashemipour, M. Mirzaee, Experimental study of influencing factors and kinetics in catalytic removal of methylene blue with TiO2 nanopowder, Am. J. Environ. Eng. 2 (2012) 1–7.

[6] R.V. Kandisa, N.S. Kv, K.B. Shaik, R. Gopinath, Dye removal by adsorption: a review, J. Bioremediation Biodegrad. 7 (2016) 1–4.

[7] N. Al-Bastaki, Removal of methyl orange dye and Na2SO4 salt from synthetic waste water using reverse osmosis, Chem. Eng. Process. Process Intensif. 43 (2004) 1561–1567.

[8] E. Alventosa-deLara, S. Barredo-Damas, M.I. Alcaina-Miranda, M.I. Iborra-Clar, Ultrafiltration technology with a ceramic membrane for reactive dye removal: optimization of membrane performance, J. Hazard. Mater. 209–210 (2012) 492–500.

[9] M. Wawrzkiewicz, Z. Hubicki, Anion exchange resins as effective sorbents for removal of acid, reactive, and direct dyes from textile, Wastewaters (2015).

[10] M. Brik, B. Chamam, P. Schöberl, R. Braun, W. Fuchs, Effect of ozone, chlorine and hydrogen peroxide on the elimination of colour in treated textile wastewater by MBR, Water Sci. Technol. J. Int. Assoc. Water Pollut. Res. 49 (2004) 299–303.

[11] S. Bai Gajbhiye, Photocatalytic degradation study of methylene blue solutions and its application to dye industry effluent, Int. J. Mod. Eng. Res. 2 (2012) 1204–1208.

[12] S. Chakrabarti, B.K. Dutta, Photocatalytic degradation of model textile dyes in wastewater using ZnO as semiconductor catalyst, J. Hazard. Mater. 112 (2004) 269–278.

[13] M. Sleiman, D. Vildozo, C. Ferronato, J.-M. Chovelon, Photocatalytic degradation of azo dye Metanil Yellow: optimization and kinetic modeling using a chemometric approach, Appl. Catal. B Environ. 77 (2007) 1–11.

[14] M.R. Hoffmann, S.T. Martin, W. Choi, D.W. Bahnemann, Environmental Applications of Semiconductor Photocatalysis, Chem. Rev. 95 (1995) 69–96.

[15] P. Borker, A.V. Salker, Photocatalytic degradation of textile azo dye over Ce1−xSnxO2 series, Mater. Sci. Eng. B 133 (2006) 55–60.

[16] J.-M. Herrmann, Heterogeneous photocatalysis: fundamentals and applications to the removal of various types of aqueous pollutants, Catal. Today 53 (1999) 115–129.

[17] A.O. Ibhadon, P. Fitzpatrick, Heterogeneous photocatalysis: recent advances and applications, Catalysts 3 (2013) 189–218.

[18] A.L. Linsebigler, G. Lu, J.T. Yates, Photocatalysis on TiO2 surfaces: principles, mechanisms, and selected results, Chem. Rev. 95 (1995) 735–758.

[19] K. Hashimoto, H. Irie, A. Fujishima, TiO2 photocatalysis: a historical overview and future prospects, Jpn. J. Appl. Phys. 44 (2005) 8269.

[20] V. Štengl, S. Bakardjieva, T.M. Grygar, J. Bludská, M. Kormunda, TiO2-graphene oxide nanocomposite as advanced photocatalytic materials, Chem. Cent. J. 7 (2013) 41.

[21] O. Carp, C.L. Huisman, A. Reller, Photoinduced reactivity of titanium dioxide, Prog. Solid State Chem. 32 (2004) 33–177.

[22] M. Behpour, M. Mehrzad, S.M. Hosseinpour-Mashkani, TiO2 thin film: preparation, characterization, and its photocatalytic degradation of basic Yellow 28 dye, J. Nanostruct.. 5 (2015) 183–187.

[23] M.A. Rauf, S.B. Bukallah, A. Hamadi, A. Sulaiman, F. Hammadi, The effect of operational parameters on the photoinduced decoloration of dyes using a hybrid catalyst V2O5/TiO2, Chem. Eng. J. 129 (2007) 167–172.

[24] H.K. Singh, M. Saquib, M.M. Haque, M. Muneer, Heterogeneous photocatalysed decolorization of two selected dye derivatives neutral red and toluidine blue in aqueous suspensions, Chem. Eng. J. 136 (2008) 77–81.

[25] H. Zhang, G. Du, W. Lu, L. Cheng, X. Zhu, Z. Jiao, Porous TiO2 hollow nanospheres: synthesis, characterization and enhanced photocatalytic properties, CrystEngComm 14 (2012) 3793–3801.

[26] W. Raza, M.M. Haque, M. Muneer, M. Fleisch, A. Hakki, D. Bahnemann, Photocatalytic degradation of different chromophoric dyes in aqueous phase using La and Mo doped TiO2 hybrid carbon spheres, J. Alloys Compd. 632 (2015) 837–844.

[27] Ö. Kerkez-Kuyumcu, E. Kibar, K. Dayıoğlu, F. Gedik, A.N. Akın, Ş. Özkara-Aydınoğlu, A comparative study for removal of different dyes over M/TiO2 (M = Cu, Ni Co, Fe, Mn and Cr) photocatalysts under visible light irradiation, J. Photochem. Photobiol. Chem. 311 (2015) 176–185.

[28] K.B. Jaimy, V.P. Safeena, S. Ghosh, N.Y. Hebalkar, K.G.K. Warrier, Photocatalytic activity enhancement in doped titanium dioxide by crystal defects, Dalton Trans. 41 (2012) 4824–4832.

[29] Ž. Antić, R.M. Krsmanović, M.G. Nikolić, M. Marinović-Cincović, M. Mitrić, S. Polizzi, M.D. Dramićanin, Multisite luminescence of rare earth doped TiO2 anatase nanoparticles, Mater. Chem. Phys. 135 (2012) 1064–1069.

[30] K.M. Joshi, V.S. Shrivastava, Removal of methylene blue dye aqueous solution using photocatalysis, Int. J. Nano Dimens. 2 (2012) 241–252.

[31] G.M. Madhu, M.L.A. Raj, K.V.K. Pai, S. Rao, Photocatalytic degradation of Orange III, Chem. Prod. Finder 25 (2006) 19–24.

[32] S.G. Poulopoulos, V.J. Inglezakis, Adsorption, Ion Exchange and Catalysis: Design of Operations and Environmental Applications, Elsevier, 2006.

Author/s:
Abdellah, MH; Nosier, SA; El-Shazly, AH; Mubarak, AA

Title:
Photocatalytic decolorization of methylene blue using TiO2/UV system enhanced by air sparging

Date:
2018-12-01

Citation:
Abdellah, M. H., Nosier, S. A., El-Shazly, A. H. & Mubarak, A. A. (2018). Photocatalytic decolorization of methylene blue using TiO2/UV system enhanced by air sparging. ALEXANDRIA ENGINEERING JOURNAL, 57 (4), pp.3727-3735. https://doi.org/10.1016/j.aej.2018.07.018.

Persistent Link:
http://hdl.handle.net/11343/230598

File Description:
Published version